

Far-infrared optical investigations on quasi-one-dimensional halogen-bridged mixed-valence compounds

L. Degiorgi and P. Wachter

*Laboratorium für Festkörperphysik, Eidgenössische Technische Hochschule Zürich–Hönggerberg,
CH-8093 Zürich, Switzerland*

M. Haruki and S. Kurita

*Laboratory of Applied Physics, Faculty of Engineering, Yokohama National University, Hodogaya-ku, Yokohama-shi,
Kanagawa-ken 240, Japan*

(Received 19 December 1988)

We have performed reflectivity measurements on one-dimensional, halogen-bridged, mixed-valence compounds, regarding, in particular, the far-infrared energy range. The ir-active phonon modes are investigated and a tentative assignment proposed, with the help of a phenomenological lattice-vibrational calculation. Furthermore, the connection between our experimental data and a theoretical model is presented, based on the Peierls-Hubbard approach.

INTRODUCTION

Compounds of the type $[M(en)_2][M(en)_2X_2](ClO_4)_4$, with $M=Pt$ or Pd , $X=Cl$, Br , or I , and $(en) \equiv$ ethylenediamine ($C_2H_8N_2$), are members of a large family of quasi-one-dimensional halogen-bridged mixed-valence insulators. Their skeletal structure consists of linear chains $—M(II)—X^— \cdots M(IV) \cdots X^—M(II)—$ of alternating metal-halogen ions, where the halogen $X^—$ ions are closer to the $M(IV)$ than to the $M(II)$ ions. Along the chain axis, each M metal ion is coordinated by four nitrogen atoms of the ethylenediamines.¹

The above mentioned displacement of the halogen ions from the midpoint results in the appearance of a commensurate charge-density wave (CDW) with a period of twice the $M-M$ separation. Thus, these chain compounds are considered a realized Peierls system. These materials, which will be abbreviated, hereafter, as MX chain, and similar ones, such as the well-known Wolfram's red salt, were intensively investigated, essentially with optical methods in the past. Reflectivity measurements in the visible and uv region and resonance Raman scattering investigations were mostly performed.²⁻⁴ Concerning the reflectivity measurements on the Pt-halogen compounds, the corresponding spectra are dominated by a peak at 2.9, 2.3, and 1.7 eV for Pt-Cl, Pt-Br, and Pt-I, respectively, when measuring with light polarized parallel to the chain axis.²⁻³ The corresponding strong absorption is ascribed to the charge-transfer (CT) transition from the d_{z^2} orbital of the $M(II)$ to the d_{z^2} orbital of the $M(IV)$, which essentially corresponds to a transition across the Peierls energy gap, formed at the edge of the folded Brillouin zone by the dimerization of the halogen $X^—$ ions. The one-electron band model determined with the aid of the tight-binding approximation confirms the above results very well.⁵

By resonance Raman scattering and luminescence experiments, Tanino and Kobayashi found as background

of a Raman line and its overtones, polarized in the chain direction and being due to a vibration along the chain, a continuous polarized Raman-like emission. It extends deeply into the band-gap and is followed by a large polarized luminescence band. They interpreted the latter features as a recombination during and after relaxation of a charge transfer excited state to the self-trapped state. These systems are, from the theoretical point of view, good prototype materials which are suitably described by the Peierls-Hubbard (PH) model. Nasu⁶ first proposed an extended version of the PH model for the MX chains.

The Hamiltonian is based on four parameters characterizing the system: the transfer energy T of an electron between two neighboring sites, the electron-phonon coupling energy S , and the intrasite and intersite electron-electron repulsive energies U and V , respectively. Considering the cooperation or the competition between the above described parameters, Wada *et al.* were able to explain the M and X dependence of the optical properties, e.g. the CT band energy of the Pt-halogen compounds,² and Tanino *et al.* described the pressure dependence of the absorption-edge of the luminescence peak and of the Raman frequency of Wolfram's red salt, as being similar to our Pt-halogen chains.⁷ More recently, Baeriswyl and Bishop also proposed a microscopic version of the PH model.⁸ Within their approach they focused their attention to the calculation of the ground state and of the configuration of the excited midgap states, due to the presence of defects, such as polaron, bipolaron, kink, or soliton. We will return to this model in more detail later in the discussion. However, we will just mention that some predictions of the theory were recently confirmed by Kurita, Haruki, and Miyagawa.⁹ In fact, they measured photoinduced absorption bands near the midgap at 77 K and identified these structures with excitations induced by metastable polaronic defects; their energy positions are in fair agreement with the theory.⁸

The motivation of our work resides in the study of the vibrational modes. The aim of the present paper is to

present our measurements in the far infrared (FIR) and near infrared (i.e., the typical energy range for ir-active phonon modes) for the whole Pt-halogen series. In particular we will try to find a possible connection between the electronic properties related to the CT band and the lattice dynamical behavior of these MX chains.

EXPERIMENT

The optical reflectivity $R(\omega)$ with light polarized perpendicular and parallel to the chain axis b of large single crystals ($2 \times 1.5 \times 1 \text{ mm}^3$) of Pt-Cl, Pt-Br, and Pt-I is measured in the energy range from 12 eV down to 1 meV at 300 and 6 K. In order to cover the whole energy range, we have made use of four spectrometers and in the FIR a Fourier spectrometer (with an energy resolution of 1 cm^{-1}) is employed with a triglycine sulfate detector down to 25 cm^{-1} and with a liquid-He-cooled Ge bolometer from 100 to 8 cm^{-1} . Furthermore, all optical properties can be obtained through Kramers-Kronig transformations of the $R(\omega)$ data.¹⁰

The single crystals were recrystallized from powder samples. The powdered material was synthesized by the procedures described in the literature.³ The recrystallization was performed in a dilute HClO_4 solution and crystals of various shapes, such as needles or platelets are grown, depending on the HClO_4 concentration. The I-compound recrystallization was performed in Japan by two of us (M.H. and S.K.), and the Pt-Cl and Pt-Br compounds were recrystallized in Zürich by E. Jilek. Only in the case of Pt-Br was the recrystallization very difficult and was the obtained shape of our single crystal smaller than usual.

RESULTS

Our thorough and complete $R(\omega)$ measurements on the whole Pt-halogen series well confirm the first and preliminary results that were partially presented in a previous paper.¹¹ Figure 1 shows the $R(\omega)$ spectra in the visi-

ble region for the three investigated systems at 300 K and for both polarization directions of the light. We can recognize the well-known CT band structure, polarized along the chain axis b . The perfect agreement with other previous and similar measurements^{2,3} confirms the good quality of our crystals and permits us to define carefully the direction of the chain axis.

We refer the reader to Refs. 3 and 5 for a detailed interpretation, based on the tight-binding calculation, of the electronic transitions. Here we point out the interesting and peculiar broad structure at 1 eV in Pt-Cl, which looks like the photoinduced midgap states detected by Kurita, Haruki, and Miyagawa⁹ or the pressure-induced band near the midgap described by Kuroda *et al.*¹² The magnitude is sample dependent but since this broad band was always detected, we have excluded that it could be due to an experimental artifact. About its origin we propose that it could be related to an absorption of midgap states, due to some intrinsic defects, e.g., of soliton- or polaron-type. In fact, the energy positions agree very well with those predicted for similar excited states within the model of Baeriswyl and Bishop⁸ (see the next section for more theoretical details). In addition, we would also like to remind the reader that similar excited midgap states were found in polyacetylene. There, the existence of a kink seems to suppress the CT absorption band.¹³ This last effect is, however, only slightly remarkable in our Pt-Cl compound. Finally, we would also like to remark that both Pt-I and Pt-Br have a slight bump at 0.5 and 0.7 eV, respectively, which we claim has the same origin as in Pt-Cl. We will return to this in a future report about the presence of defects in these Pt-halogen chains.

Let us now move to the far-infrared (FIR) results, which are, to our knowledge, presented here for the first time. From Figs. 2–9 we present the spectra for both polarizations of light and temperatures of the three Pt-halogen compounds. Once again, a huge anisotropy between the two polarization directions characterizes the spectra of all samples. The Pt-Cl and Pt-Br $R(\omega)$ spectra

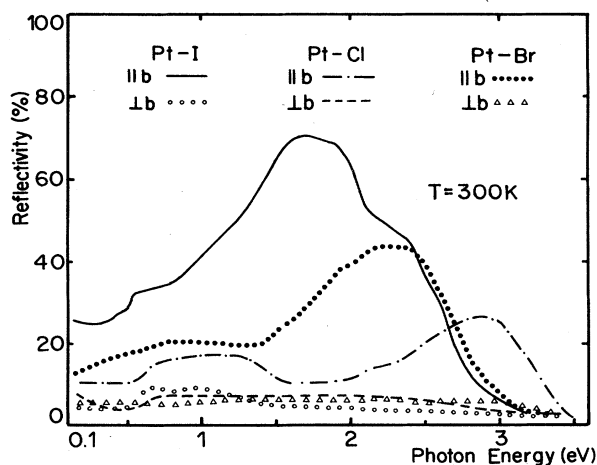


FIG. 1. $R(\omega)$ at 300 K between 0.1 and 3.6 eV for Pt-Cl, Pt-Br, and Pt-I with light polarized parallel and perpendicular to b .

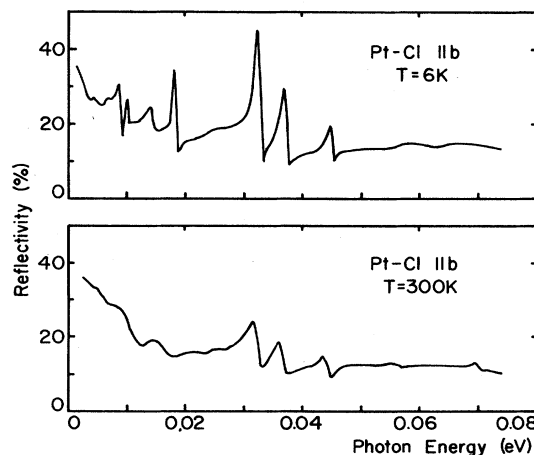


FIG. 2. FIR- $R(\omega)$ at 300 K and 6 K for Pt-Cl, with light polarized parallel to b .

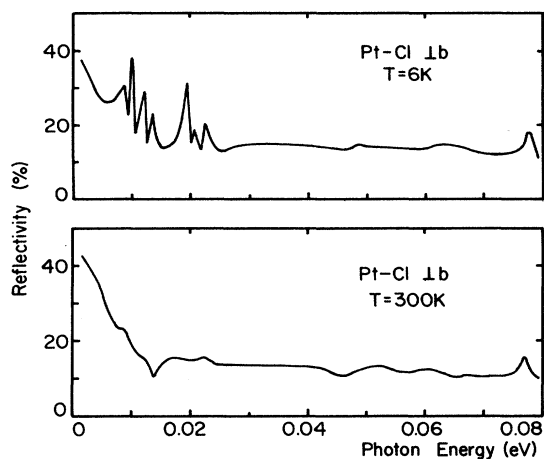


FIG. 3. FIR- $R(\omega)$ at 300 K and 6 K for Pt-Cl, with light polarized perpendicular to b .

(Figs. 2–5) are dominated by four mode structures along the chain axis, which grow up with decreasing temperature, accompanied sometimes by a typical splitting at low temperatures. The Pt-I spectra (Figs. 6–9), however, are more complex and rich in structure. The equivalent four modes in Pt-I are identified among the other structures (see arrows), comparing the shape and form, and the relative intensity with the corresponding four ones in Pt-Cl and Pt-Br. We attempt to assign the other structure modes in Pt-I to the internal vibrational states of the planar (en) complexes and of the interchain (ClO_4) molecules.¹⁴ Since the purpose of this work resides in the study of the phonon modes along the chain axis, a detailed investigation and assignment of the ir-active phonons of the planar (en) and (ClO_4) molecules goes beyond the aim of the present discussion. It is our intention to devote a future work to this problem. However, we guess that the reason for such differences between the spectra

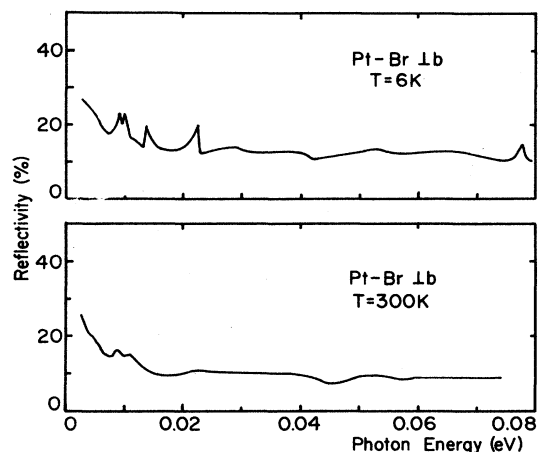


FIG. 5. FIR- $R(\omega)$ at 300 K and 6 K for Pt-Br, with light polarized perpendicular to b .

of Pt-I and those of Pt-Cl and Pt-Br resides in the higher stability and purity of the former. In fact, the recrystallization for the latter two compounds essentially follows from an alignment of many needles along the main axis. Of course this alignment is not always perfect and, as a consequence, this could produce smearing and broadening effects. This is seen well just in the $R(\omega)$ spectra, where for Pt-I the mode structures appear more intensive than in Pt-Cl or Pt-Br. Before concluding this section, we wish to consider another interesting aspect which manifests itself by close inspection of the spectra: namely, the appearance of new modes by lowering the temperature and this for both polarization directions of light. Cooling down the samples, some internal distortions (e.g., a zig-zag behavior of the b axis) could happen and consequently new ir-active modes arise, due to a break in the symmetry. However, we do not know at the present time of any neutron diffraction experiment which would confirm our guess.

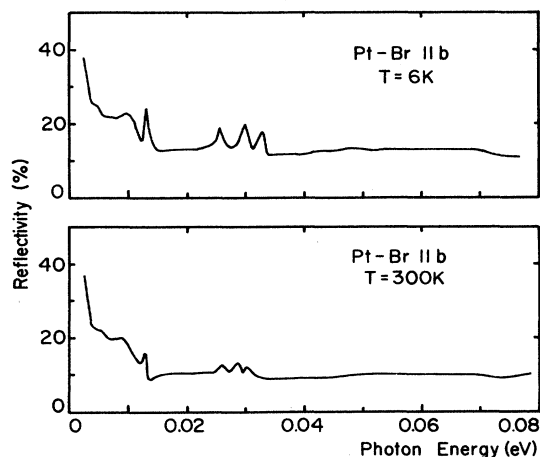


FIG. 4. FIR- $R(\omega)$ at 300 K and 6 K for Pt-Br, with light polarized parallel to b .

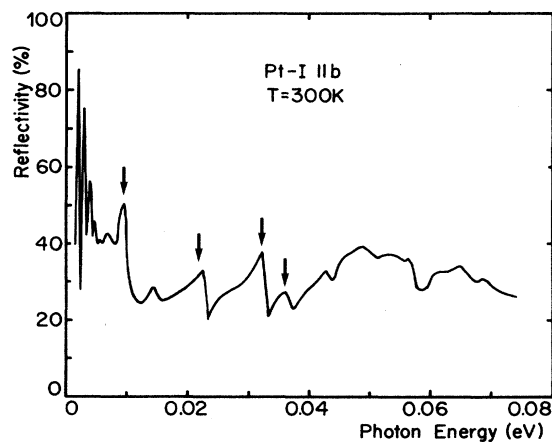


FIG. 6. FIR- $R(\omega)$ at 300 K for Pt-I, with light polarized parallel to b .

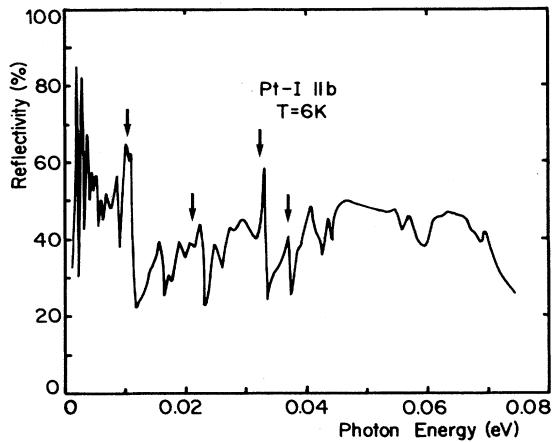


FIG. 7. FIR- $R(\omega)$ at 6 K for Pt-I, with light polarized parallel to b .

DISCUSSION

As pointed out in the previous section, the common features which characterize the $R(\omega)$ spectra of the three investigated Pt-halogen compounds concern, above all, the four highly polarized mode structures along the b axis. Since in the following discussion we will concentrate on the assignment and interpretation of these modes, we have summarized *for the sake of clarity*, the experimental data in Table I. The mode frequencies are taken from the imaginary part of the dielectric constant ϵ_2 .

First of all, in view of the main purpose of our discussion we propose a pertinent and interesting comparison between the FIR spectra of our systems and the corresponding one of $\text{BaBi}_{1-x}\text{Pb}_x\text{O}_3$. It is, in fact, or intention to propose, as it will become clear just below, the dynamical similarity of the two systems. This compound forms an apparently complete solid solution with perovskite-type structure in the entire range $0 < x < 1$.

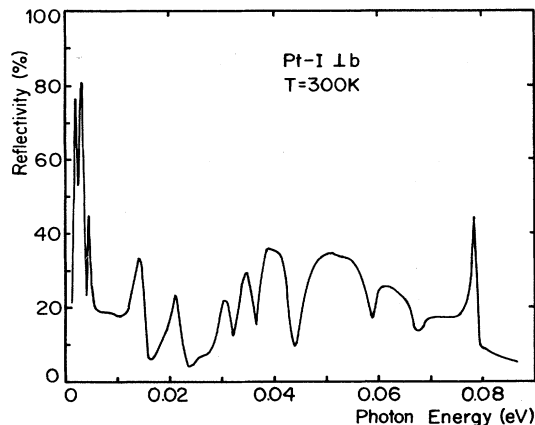


FIG. 8. FIR- $R(\omega)$ at 300 K for Pt-I, with light polarized perpendicular to b .

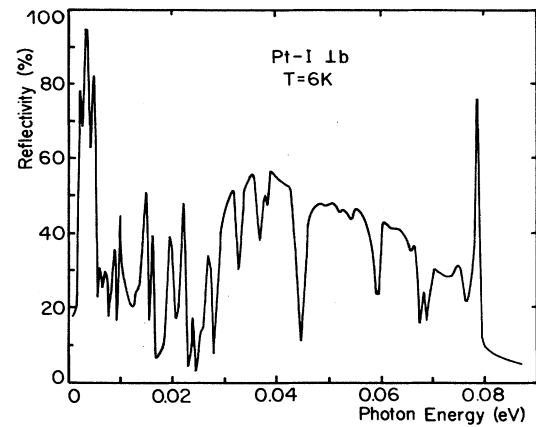


FIG. 9. FIR- $R(\omega)$ at 6 K for Pt-I, with light polarized perpendicular to b .

The perovskite structure consists of a three-dimensional array of oxygen octahedra, either Pb or Bi atoms being located at the center of each octahedra. Furthermore, in the whole semiconducting phase ($x \leq 0.35$) a charge disproportionation (which is progressively destroyed by alloying with Pb) on the Bi atoms exists, leading to a mixed-valence ground state.

By considering one crystallographic direction of the isotropic perovskite structure, we obtain a chain of alternating Bi and/or Pb—O ions, where each Bi and/or Pb ion is coordinated by four O ions in a plane perpendicular to the Bi and/or Pb chain. In other words, the structure along such directions is similar to a chain of O-corner-sharing octahedra with Bi and/or Pb ions in their center. Then, even though the Ba-Bi-Pb-O compound is three dimensional, it is quite easy to convince oneself that, from the dynamical point of view, our Pt- X are totally equivalent to Ba-Bi-Pb-O, and it is not surprising that the same ir-active structures appear. In fact, Uchida *et al.*¹⁵ measured the FIR $R(\omega)$ of the former system in the semiconducting phase ($x \leq 0.35$) and they found a similar

TABLE I. (a) Frequencies of the four modes along the b axis for the three Pt-halogen compounds. The values are in meV. (b) Energy of the CT band (i.e., the optical gap E_g^{opt}) and of the transfer integral t_0 (i.e., the width of the CT band). The values are in eV.

	(a)			
	$\bar{\omega}_1$	$\bar{\omega}_2$	$\bar{\omega}_3$	$\bar{\omega}_4$
Pt-Cl	14.9	31	36	43.4
Pt-Br	13.6	25.4	30	33
Pt-I	9.3	21.7	31.6	36
	(b)			
	Pt-Cl	Pt-Br	Pt-I	
E_g^{opt}	2.9	2.3	1.7	
t_0	0.7	1.1	1.5	

phonon spectrum dominated by four structures. The four structures in Ba-Bi-Pb-O are assigned to three internal modes (i.e., concerning atom movements within the oxygen octahedra) and to an external one (i.e., where the cubic lattice formed by the Ba atoms moves against the whole oxygen octahedra).¹⁵

Due to the analogies pointed out thus far, we will go further and develop the same interpretations and kind of analysis proposed by Uchida *et al.*¹⁵ for the Ba-Bi-Pb-O system, for our *MX* chains. We will perform a phenomenological calculation based on the linear harmonic oscillator model. Following Fig. 10, we will take our Pt-halogen compound as a one-dimensional two-atom base chain. From the CDW ground state the dimerized unit cell $\text{Pt(III}+\delta\text{)}\text{-X}^-\text{-Pt(III}-\delta\text{)}\text{-X}^-$ follows (where $0 < \delta < 1$ describes the charge disproportion), which, along the chain, contains four atoms. Then, to each Pt ion is attached a (en) planar molecule, which is modeled by four out-of-chain bendings; each of them is formed by a complex with the total mass of C and N atoms (Fig. 10) (i.e., in the case of Ba-Bi-Pb-O, instead of halogen and C-N complexes there are oxygen atoms and instead of Pt there are Bi and/or Pb atoms).

In order to calculate the vibrational modes in the linear harmonic approximation, we consider two types of interactions: the in-chain stretching distortions with the spring force constants K_i and the out-of-chain bending distortions with the spring force constant K'_i , where $i=1,2$ indicates the Pt ions with $3+\delta$ and $3-\delta$ charge disproportion (Fig. 10). The unit cell then contains a total of 12 atoms and a 12×12 dynamical matrix D_{ij} follows (see Appendix for more in depth details). Solving the corresponding determinantal equation,

$$|D_{ij} - M_{ij}\omega_n^2\delta_{ij}| = 0, \quad (1)$$

we determine the eigenfrequencies ω_n . From the 12 eigenfrequencies, one corresponds to the zero-frequency acoustic mode (inactive), three to the ir-active modes and the other eight to the Raman-active modes. In fact, the ir phonons can be assigned to the stretching mode, where

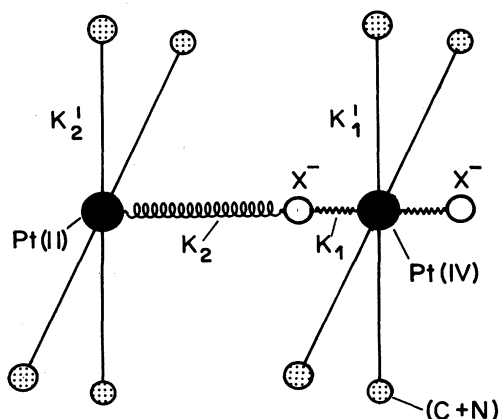


FIG. 10. Unit cell of Pt-halogen chains, considered for the phenomenological fit (see text).

the Pt ions and the *X* ions move in the opposite direction to the zone-boundary acoustic mode as a result of the Brillouin-zone folding and (finally, because we also consider the bending interactions) to the so-called ir bending mode. Among the Raman-active modes we find the typical breathing phonon modes, where the halogens move against the Pt ions and the sevenfold-degenerate bending modes, involving essentially the (C—N) complexes which model the (en) molecules (see Fig. A.3 of Ref. 15).

We now have to find the best set of the parameters K_i and K'_i ($i=1,2$) in order to obtain the best possible fit with the experimental values. The results of our fitting procedure is summarized in Table II, which shows the good agreement between the experimental and calculated modes. We would like to remind the reader that we have exposed the eigenfrequencies (calculated and experimental) for each Pt-halogen compound in Table IIb in the increasing energy order. We note that the fit considers only the structural modes at 300 K, since the temperature dependence is negligible. The differences between the calculated and the experimental values (except for the higher mode in Pt-Br) oscillate between 0.6 and 2.5 meV. This numerical imprecision is of the same order of magnitude as the shift measured in the Raman breathing mode, when exciting with light of different energies. Without going into detail, it was suggested that the dispersion of the Raman breathing mode frequency with change of the wave number of the excitation light depends on the extent of the valence delocalization along the chain.¹⁶ From the calculation of the eigenstates, we can assign the lowest frequency ir mode to the zone-boundary acoustic mode, which is expected, since the reduced mass of this mode is equal to the Pt ion mass. Furthermore, the vibrational states at 43.4, 25.4, and 21.7 meV for Pt-Cl, Pt-Br, and Pt-I respectively, are assigned to the ir-active stretching mode and the phonon states at 36 meV for the Pt-Cl and Pt-I and at 33 meV for Pt-Br to the ir-active bending mode. The halogen independent mode at 26 meV corresponds to the Raman-active bending mode, as Tanino *et al.*¹⁷ found by Raman measurements in Pt-(Cl_{1-x}Br_x) mixed halogen compounds. The halogen independence of this sevenfold-degenerate mode follows from the fact that only the (en) complexes are involved but the Pt and halogen ions do not move at all. This is well confirmed, also, by our calculations, which demonstrate that the mode frequency depends only on K'_i . Furthermore, the numerical values of the K'_i constants are quite the same for the whole Pt halogen series. The small differences account for the different δ disproportion on the Pt ions and consequently for the small experimental dispersion of this ir-active bending mode.¹⁷ Regarding the Pt-I compound, we have not found any experimental results for this ir bending mode. However, from the above considerations, we have to expect an experimental frequency of about 26 meV, as predicted by our calculation. The modes at 38.5, 21.5, and 15.4 meV correspond to the Raman breathing mode for Pt-Cl, Pt-Br, and Pt-I, respectively.¹ With the described phenomenological approach, we can only consider the so-called internal modes. However, our ir spectra are characterized by a fourth structure (i.e., at 31, 30, and 31.6 meV

TABLE II. Spring force constants K_i and K'_i (with $i=1,2$) used in the phenomenological fit, experimental and calculated phonon frequencies (ω_n) and the parameters within the PH model: the spring force constant K (within brackets the unscreened \bar{K} for Pt-I and Pt-Br), the dimensionless parameter λ_2 , and the electron-phonon coupling constant β .

	K_1 (mdyn/Å)	K_2 (mdyn/Å)	K'_1 (mdyn/Å)	K'_2 (mdyn/Å)	ω_1 (meV)		ω_2 (meV)		ω_3 (meV)		ω_4 (meV)		ω_5 (meV)	
					expt.	calc.	expt.	calc.	expt.	calc.	expt.	calc.	expt.	calc.
Pt-Cl	1.10	0.87	0.658	0.021										
Pt-Br	0.84	0.6	0.58	0.06										
Pt-I	0.73	0.61	0.66	0.01										
	K (mdyn/Å)	(\bar{K}) (mdyn/Å)	λ_2	β (eV/Å)										
Pt-Cl	0.985		0.413	2.36										
Pt-Br	0.72	(1.46)	0.25	2.81										
Pt-I	0.67	(1.77)	0.19	3.14										

^aThis work, Table I(a).

^bReference 1.

^cReference 15.

for Pt-Cl, Pt-Br, and Pt-I, respectively) which we have assigned to an ir mode of external type (also proposed by Uchida *et al.* for the Ba-Bi-Pb-O¹⁵). This external mode involves the whole Pt-*X* chain against the interchain complexes formed by the (ClO₄) molecules. The fact that the reduced mass of this mode is essentially equal to the total mass of the (ClO₄) molecule for the whole Pt-halogen series, supports the experimental evidence of finding the external mode at the same frequency for all Pt compounds. Another interesting feature which evolves from Table II is the tendency to reach the best fit with constants K_1 and K_2 , which do not appreciably differ from each other. This is more and more pronounced going from Pt-Cl to Pt-Br, and to Pt-I. The progressive leveling of K_1 and K_2 is in contrast to the numerical conclusions proposed by Clark¹ who considered only the interactions within the chain (i.e., this will reduce the dimension of the dynamical matrix to four, see Appendix). In fact, K_1 differs about a factor between 10 and 20 from K_2 .¹⁸ It appears to us that this large difference is to be ascribed to a certain renormalization due to the omission of the out-of-chain bending interactions. However, the small and increasing (from Pt-I to Pt-Cl) difference between K_1 and K_2 in our fit accounts for the δ charge disproportion on the Pt site, likewise as the K'_i constants.

Before concluding, we will explore possible connections between the experimental and theoretical investigations. As mentioned in the Introduction, these systems are considered suitably within the Peierls-Hubbard model. Baeriswyl and Bishop⁸ considered within their approach an undistorted single chain, consisting of a sequence of *M* and *X* atoms, where the neighboring elastic lattice interactions are modeled in terms of a harmonic

spring constant K . In addition to the elastic energy term, the Hamiltonian assumes a single tight-binding form for the electronic energy states on the Pt sites and the charge-transfer term between two nearest-neighbor Pt ions. The electronic energy levels ε_n are expected to depend sensitively on the position v_n of the neighboring halogen ions, whereas the resonance integral $t_{n,n+1}$ for the charge-transfer will be a function of the distance between the nearest-neighbor Pt ions. The dependence is assumed to be linear through the electron-phonon coupling constants α and β , respectively. Two competing instabilities are then considered: one associated with alternating bond lengths $u_n = (-1)^n \bar{u}$ inducing a bond-order wave (BOW), or the other one associated with the displaced *X* atoms $v_n = (-1)^n \bar{v}$ leading to a CDW ground state. In the CDW limits ($\bar{u} = 0, \bar{v} \neq 0$), which is interesting for our systems, the gap E_g of the electronic density of states is then equal to $4\beta\bar{v}$ (i.e., \bar{v} describes the dimerization of the halogen ions against the Pt ones). Baeriswyl and Bishop proposed to evaluate the spring constant K from the expression $\omega_o^2 = 2K/\bar{M}$ for the Raman breathing mode, where \bar{M} is the halogen atomic mass. However, within our phenomenological approach, we know that $\omega_o^2 = (K_1 + K_2)/\bar{M}$, where K_1 and K_2 are different due to the dimerized unit cell. This is not surprising because the squared frequency of the Raman breathing mode is the same for an harmonic oscillator around the equilibrium position as for a displaced one,¹⁹ i.e., when an harmonic oscillator reaches a new equilibrium position, this only lowers the zero-point energy.

This exact theoretical result should not confuse the reader, in the sense that one might be encouraged to develop the phenomenological fit with the condition

$K_1=K_2=K$. In fact, one has to keep in mind that, in the approach of Baeriswyl and Bishop,⁸ the starting point is an *undistorted* chain, where the dimerization is an effect of the electron-phonon coupling. In our approach, where we do not consider the electron-phonon coupling explicitly, the double unit cell, due to the dimerized CDW ground state, implies $K_1 \neq K_2$. From the above discussion we can extract the spring force constant K of Baeriswyl and Bishop⁸ from the relation $2K = K_1 + K_2$. From our best numerical calculations, $K_1 + K_2$ is approximately equal to $2K$, obtained directly from the Raman frequency. In Table II we summarize the K values and the electron-phonon coupling constants for the three Pt halogen compounds.

For Pt-Cl we can calculate the coupling constant from the equation $\bar{v} = \beta/K$; for a dimerization $\bar{v} = 0.384 \text{ \AA}^1$ we obtain $\beta = 2.4 \text{ eV \AA}^{-1}$ which seems a quite reasonable value.⁸ A calculated electronic gap of 3.62 eV then follows, which is larger by about 0.725 eV than the measured optical gap. This difference is ascribed to the Coulomb interactions. One can enlarge the Hamiltonian, by introducing the on-site Coulomb interaction U , which will destroy the CDW state, and the intersite Coulomb interaction V , which will favor the CDW state. In the classical limit characterized by a strong coupling, which manifests itself by an integer or a quite complete charge disproportion, the optical gap satisfies the relation: $E_{\text{opt}} = E_g + 3V - U$, where $E_g = 4\beta\bar{v}$. Then we assign the above mentioned difference between E_{opt} and E_g to $U - 3V$. For the Pt-Br and Pt-I compounds the so-called weak-coupling limit was proposed.⁸ In fact, due to the extended nature of the wave functions, the electron transfer between the p_z of X^- and the d_{z^2} of Pt^{3-6} increases in these compounds. Besides the halogens are pulled towards the Pt^{3-6} ions, and thus the amplitude of the CDW, optical gap energy and Peierls distortion will decrease.¹⁻⁴ The huge overlap between the orbitals involved in the transfer (or supertransfer) process produces a screening effect of the lattice interactions. One has to then consider a renormalized spring force constant. It follows for the Raman frequency $\omega_0^2 = 2\lambda_2(2\bar{K}/\bar{M})$ and for the electronic gap $E_g = 4\beta\bar{v} = 16t_0 \exp[-(2\lambda_2)^{-1}]$,⁸ where \bar{K} is the unscreened spring force constant, t_0 is the transfer integral, and λ_2 is the dimensionless parameter $\beta^2/(\pi t_0 \bar{K})$. Neglecting the Coulomb interactions, which would modify the analysis somewhat,²⁰ and defining $E_{\text{opt}} = E_g$, we can calculate from the above formula the parameter λ_2 which takes the values 0.25 and 0.19 for Pt-Br and Pt-I, respectively. Considering once again the relation $2K = K_1 + K_2 = 2\lambda_2(2\bar{K})$, we can calculate the screened K parameter from the experimentally fitted spring force constants. In Table II, in addition to the screened spring force constants K , we have also summarized in brackets the values of \bar{K} for the Pt-Br and Pt-I compounds.

From the width of the CT absorption band in $R(\omega)$ we can estimate t_0 , and returning back to the expression for the electronic gap in the weak-coupling limit, we can finally calculate the theoretical dimerization \bar{v} . For the Pt-I we obtain $\bar{v} = 0.135 \text{ \AA}$ and for Pt-Br $\bar{v} = 0.205 \text{ \AA}$,

which for the Pt-I compound agrees very well with the experimental value of 0.123 \AA .¹ For the Pt-Br compound, however, we have not found a reasonable experimental value for \bar{v} . In fact, the value reported by Clark,¹ after the work of Endres *et al.*,²¹ is in striking contradiction with the tendency manifest by other similar Pt-Br compounds, where in place of (en) one has trimethylenediamine (tn), propylenediamine (pn) etc. complexes (see Table III of Ref. 1). A useful quantity in this context is the ratio ρ between the Pt(II)-Br and the Pt(IV)-Br distances. Taking then an average Pt-Pt distance of 5.48 \AA and our \bar{v} theoretical value we reach a $\rho = 0.86$, which is now more consistent than the 0.98 value of Ref. 21, derived with a \bar{v} ten times smaller! As final remark in this part of the discussion, we would like to point out that within the model of Baeriswyl and Bishop,⁸ the experimental value of \bar{v} proposed by Endres *et al.*,²¹ would imply in the weak-coupling limit an electronic gap of 0.3 eV. The huge discrepancy with the experimental optical gap could only be explained, by no longer considering Pt-Br in the Peierls CDW limit but instead as an exponent of the Mott Hubbard limit. E_g^{opt} is then a correlation gap, due to the important Coulomb correlation energy. However, this does not seem to be very realistic in comparison with the other two Pt-Cl and Pt-I compounds, and we then attribute the apparent discrepancy of \bar{v} to an experimental artifact.²² Regarding the electron-phonon coupling constant β , summarized in Table II, it seems, once again, to be quite consistent.⁸

We will end our discussion by pointing out the trend, outlined before, for the spring force constants K_1 and K_2 of assuming approximately the same value. This aspect confirms phenomenologically the weak-coupling limit nature of the electron-phonon interaction, which also implies a smaller charge disproportion contrary to the case of Pt-Cl. Due to the above cited tendency, and since all modes depend on $K_1 \pm K_2$ and on $K'_1 \pm K'_2$ it is not surprising that, for the Pt-halogen in the weak-coupling limit, we can reach a quite good fit of the whole phonon spectra, imposing the condition $K_1 = K_2$. About the charge disproportion, we finally remark that it is possible to perform a preliminary calculation of the effective charges on the halogen ions, starting from the ω_{TO} and ω_{LO} phonon modes, as proposed by the procedure of Scott and Gervais.¹⁵ The ω_{TO} frequencies are extracted from $\epsilon_2(\omega)$ and the ω_{LO} from the energy loss spectra. We remark, with quite good accuracy, that the effective charge on the halogen ions diminishes progressively from the Cl down to the I and Br compounds, indicating so far that the ionicity of the Pt-halogen bonding decreases, going from compounds of strong to those of weak-coupling electron-phonon interaction.

CONCLUSION

We have presented our thorough FIR $R(\omega)$ spectra of the Pt-halogen chains by concentrating our effort on the interpretation of the phonon structures. In fact, in addition to the similarity of our spectra with Ba-Bi-Pb-O, which also implies a dynamical equivalence, we have assigned, based on a phenomenological model, the four

detected modes along the b axis to three vibrational states of internal type and one to a phonon state of external type. It was then possible to find a connection between the lattice dynamical properties and the electronic ones, within the so-called PH model. We have discussed our numerical results concerning the spring force constants, as input parameters for the calculation of the optical gap and the dimerization, as a consequence of the realized Peierls ground state. Finally, as briefly mentioned in the previous discussion, the PH model of Baeriswyl and Bishop predicts the midgap state energies, for soliton, polaron, and bipolaron defects,⁸ the existence of which was recently demonstrated in Pt-Cl by Kurita, Haruki, and Miyagawa.⁹ It is our future purposal to perform photoinduced FIR $R(\omega)$ measurements in order to study the phonon modes around such defects. Furthermore, the FIR study of Pt mixed-halogen compounds would be of great interest in order to consistently investigate the effect of the d orbital states extension of the Pt ions on the phonon modes.

ACKNOWLEDGMENTS

The authors are grateful to Dr. D. Baeriswyl, Dr. A. R. Bishop, Dr. R. Monnier, and Dr. B. I. Swanson for

stimulating discussions and to E. Jilek, J. Müller, and H. P. Staub for technical assistance.

APPENDIX

To get quantitative insight into the internal phonon modes we have proposed a phenomenological lattice-vibrational calculation based on the linear harmonic approximation. The situation pointed out in Fig. 10 is considered for the unit cell. Here, we will concentrate on the formal aspects of the calculation following the approach of Uchida *et al.*¹⁵

We are interested only in the zone-center ($\mathbf{k}=\mathbf{0}$) modes of the folded Brillouin zone which are relevant for the ir spectra. The equation of motion, taking in consideration a one dimensional space, is then

$$M_i \omega^2 u_i = \sum_j D_{ij} u_j, \quad (\text{A1})$$

where M_i is the mass of the i th atom and u_i is the one-dimensional Cartesian component of the i th-atom displacement from its equilibrium position. Remembering that only a nearest-neighbor force constant is taken into account, the dynamical matrix follows:

$$D_{ij} = \begin{pmatrix} 2K_1 + 8K'_1 & 0 & -K_1 & -K_1 & -K'_1 & \cdots & -K'_1 \\ 0 & 2K_2 + 8K'_2 & -K_2 & -K_2 & -K'_2 & \cdots & -K'_2 \\ -K_1 & -K_2 & K_1 + K_2 & 0 & 0 & \cdots & 0 \\ -K_1 & -K_2 & 0 & K_1 + K_2 & 0 & \cdots & 0 \\ -K'_1 & -K'_2 & 0 & 0 & K'_1 + K'_2 & 0 & 0 \\ \vdots & \vdots & \vdots & \vdots & 0 & \ddots & 0 \\ -K'_1 & -K'_2 & 0 & 0 & 0 & 0 & K'_1 + K'_2 \end{pmatrix}. \quad (\text{A2})$$

The normal modes are given by the solutions of the equations:

$$\sum_j D_{ij} u_j^{(n)} = \omega_n^2 M_i u_i^{(n)}, \quad (\text{A3})$$

where $u_i^{(n)}$ represent the displacement of the i th atom of the n th normal mode. The corresponding eigenvalues

problem is considered in the discussion. Finally, we recall that without the out-of-chain bending interactions (i.e., $K'_i=0$, $i=1,2$), the dynamical matrix reduces its dimension to four and would correspond to the 4×4 matrix in the upper left-hand corner. This is exactly the approach considered by Clark.¹

¹R. J. H. Clark, in *Advances in Infrared and Raman Spectroscopy*, edited by R. J. H. Clark and R. E. Hester (Wiley, New York, 1984), Chap. 3, p. 95, and references therein.

²Y. Wada, T. Mitani, M. Yamashita, and T. Koda, *J. Phys. Soc. Jpn.* **54**, 3143 (1985).

³M. Tanaka, S. Kurita, T. Kojima, and Y. Yamada, *Chem. Phys.* **91**, 257 (1984).

⁴H. Tanino and K. Kobayashi, *J. Phys. Soc. Jpn.* **52**, 1446 (1983).

⁵M. Tanaka, S. Kurita, M. Fujisawa, and S. Matsumoto, *J. Phys. Soc. Jpn.* **54**, 3632 (1985).

⁶K. Nasu, *J. Phys. Soc. Jpn.* **52**, 3865 (1983).

⁷H. Tanino, N. Koshizuka, K. Kobayashi, M. Yamashita and K. Hoh, *J. Phys. Soc. Jpn.* **54**, 483 (1985).

⁸D. Baeriswyl and A. R. Bishop, *J. Phys. C* **2**, 339 (1988).

⁹S. Kurita, M. Haruki, and K. Miyagawa, *J. Phys. Soc. Jpn.* **57**, 1789 (1988).

¹⁰G. Travaglini, Ph.D. thesis, Eidgenössische Technische Hochschule, Zurich, No. 7687 (1985).

¹¹L. Degiorgi, P. Wachter, M. Haruki, and S. Kurita, in *Proceedings of the International Conference on Science and Technology of Synthetic Metals (ICSM '88)*, Santa Fe, 1988,

- edited by M. Aldissi [Synth. Met. **29**, F137 (1989)].
- ¹²N. Kuroda, M. Sakai, Y. Nishina, M. Tanaka, and S. Kurita, Phys. Rev. Lett. **58**, 2122 (1987).
- ¹³N. Suzuki, M. Ozaki, S. Etemad, A. J. Heeger, and A. G. MacDiarmid, Phys. Rev. Lett. **45**, 1209 (1980).
- ¹⁴G. Zerbi (private communication).
- ¹⁵S. Uchida, S. Tajima, A. Masaki, S. Sugai, K. Kitazawa, and S. Tanaka, J. Phys. Soc. Jpn. **54**, 4395 (1985).
- ¹⁶R. J. H. Clark and M. Kurmoo, J. Chem. Soc. Faraday Trans. 2 **79**, 519 (1983).
- ¹⁷H. Tanino, K. Takahashi, M. Kato, and T. Yao, Solid State Commun. **65**, 643 (1988).
- ¹⁸The K_1 and K_2 values of Clark (Ref. 1) are taken as starting parameters of our fit procedure.
- ¹⁹H. Haken, *Quantum Field Theory of Solids* (North-Holland, Amsterdam, 1976), Chap. 2, p. 40.
- ²⁰S. D. Conradson, M. A. Stroud, M. H. Zietlow, B. I. Swanson, D. Baeriswyl, and A. R. Bishop, Solid State Commun. **65**, 723 (1988).
- ²¹H. Endres, H. J. Keller, R. Martin, U. Traeger, and M. Novotny, Acta Crystallogr. B **36**, 35 (1980).
- ²²B. I. Swanson (private communication).